A Study of Pyruvate-Induced Inhibition in the Dogfish Lactate Dehydrogenase System. Mechanistic Comparison with the Iodination of Pyruvate†

John W. Burgner, II,* and William J. Ray, Jr.‡

ABSTRACT: The complex of NAD^+ with a subunit of dogfish M_4 lactate dehydrogenase reacts with pyruvate in neutral, aqueous solution to produce an inactive, adduct complex; in the adduct a covalent bond has formed between the nicotinamide ring and the pyruvate moiety (see Everse, J., Barnett, R. E., Thorne, C. J. R., and Kaplan, N. O. (1971), *Arch. Biochem. Biophys. 143,* 444). The effects of enzyme and buffer concentration on the rate of the adduct reaction (ionic strength = 0.2) were measured spectrally at saturating NAD^+: λ_{max} 325 nm; ϵ_{max} 7700 M^{-1} cm^{-1} for the adduct complex. This reaction bears a marked resemblance to the reaction of iodine with pyruvate, except that the bond-forming step in the iodination is considerably faster than the corresponding step in the adduct reaction. Thus, both iodination and adduct formation require the enol form of pyruvate as a reactant. Because of this, iodination is zero order in $[I_2]$ and adduct formation approaches zero order in $[E{\cdot}NAD^+]$ at high concentrations of the latter. In addition iodination rates are buffer sensitive to the extent that general base catalysis facilitates the enolization step. The adduct reaction is similarly sensitive to buffer catalysis, and values of rate constants both for the "uncatalyzed" and phosphate-catalyzed enolizations of pyruvate are essentially the same when calculated from data obtained from either iodination or adduct formation. However, in contrast to iodination, the *order* of the adduct reaction varies with buffer concentration—as well as with $E{\cdot}NAD^+$ concentration—at intermediate concentrations of both, and approaches a first-order process in $[E{\cdot}NAD^+]$ at high concentrations of buffer and low concentrations of $E{\cdot}NAD^+$. An explanation of this behavior is given in terms of the relative rates of keto-enol interconversion and covalent bond formation as well as the effect of buffer catalysis on the former step. Previous *in vitro* studies are considered in view of these observations.

Substrate inhibition of LDH[1] from the heart and muscle tissue of many different vertebrates, at pyruvate concentrations greater than its Michaelis constant, is well documented (see Everse and Kaplan, 1973). In the reverse reaction (pyruvate + NADH → lactate + NAD^+), such inhibition produces a decrease in velocity with increasing pyruvate concentration above a certain minimum. Novoa *et al.* (1959) initially suggested that this inhibition was caused by formation of a dead-end, "ternary" complex: $E{\cdot}NAD{\cdot}Pyr_K$, while subsequent studies indicated that inhibition was produced by the enzymic formation of a tightly bound inhibitor in which the β-carbon of pyruvate is covalently joined to the 4 position of the nicotinamide ring, *i.e.*, an $E{\cdot}NAD^+$–Pyr adduct complex[2] (Lee *et al.*, 1965, 1966; DiSabato, 1968; Gutfreund *et al.*, 1968; Everse *et al.*, 1971a). However, recognition of the possibility that *both* types of inhibition may occur has not been widespread. Although the present paper deals primarily with the adduct reaction, a subsequent paper will consider both possibilities in greater detail (see also the Discussion section).

Two different mechanisms have been suggested for the formation of the NAD–Pyr adduct. Griffin and Criddle (1970) propose a reaction sequence which involves dissociation of the LDH tetramer to the monomer, followed by reaction of the monomer with NAD^+ and pyruvate. This mechanism is based on their observation that whereas the adduct reaction is first order with respect to [LDH] at low enzyme concentrations, the order decreases with increasing [LDH] to quarter order, which would be the expected order when the tetramer predominates over the monomer by many fold, if the monomer, alone, were active. However, no independent evidence is available to demonstrate that dissociation of the LDH tetramer is sufficiently rapid at neutral pH and room temperature to support this mechanism. As an alternative, Sugrobova *et al.* (1972) propose a mechanism in which the enol form of pyruvate binds to $E{\cdot}NAD^+$ to form a ternary complex followed by conversion of the ternary complex to the adduct complex in what appears to be a rate-limiting step. This mechanism was supported by the claim that the initial velocity of the adduct reaction actually is a hyperbolic function of the enzyme concentration. Since a hyperbolic relationship between the initial velocity and enzyme concentration also could be caused by a change in the identity of the rate-determining step from covalent bond formation at low enzyme concentration to enolization of pyruvate at high concentrations of enzyme, as opposed to the proposed saturation phenomenon, we have investigated the effect of buffers on the rate of the adduct reaction.

Theory

The reaction of pyruvate with $LDH(NAD^+)_4$ produces 1 mol of adduct/mol of subunit (DiSabato, 1968; Everse *et al.*,

† From the Department of Biological Sciences, Purdue University, West Lafayette, Indiana 47907. *Received May 3, 1974.* This investigation was supported by research grants from the National Institutes of Health (GM08963) and the National Science Foundation (GB219273X), and by a predoctoral Training Grant from the National Institutes of Health (GM00779).

‡ National Institutes of Health Career Development Awardee.

[1] Abbreviations used are: LDH, lactate dehydrogenase (the dogfish M_4 enzyme, unless otherwise indicated); E, a subunit of the LDH tetramer (see Theory section); Pyr, pyruvate; Pyr_K and Pyr_E, the keto and enol forms of pyruvate, respectively; NAD–Pyr or adduct, the covalent addition product or products of nicotinamide adenine dinucleotide and pyruvate generated by LDH (see Results section and footnote 7).

[2] Since the expression "abortive ternary complex" frequently has been used as a general description for complexes with the stoichiometry, enzyme plus product–coenzyme plus reactant–substrate, without regard to the chemical nature of these complexes, this term is not used here. Instead we use E·NAD–Pyr or adduct complex, a "binary" complex of an LDH subunit, NAD^+, and pyruvate.

1971a). Since the preponderance of evidence indicates that the four catalytic sites of LDH are equivalent and independent (Holbrook and Gutfreund, 1973; Burgner, 1973), [E·NAD$^+$] will be used herein to refer to the concentration of catalytic sites containing coenzyme. Since there is no evidence for the presence of free monomers under the conditions of our experiments (see Discussion), presumably E·NAD$^+$ is present only as one of the subunits in a tetramer.

As pointed out above, the enol form of pyruvate probably reacts with E·NAD$^+$ to produce the inactive enzyme-adduct complex

$$\mathrm{Pyr_K} \underset{k_2}{\overset{k_1}{\rightleftharpoons}} \mathrm{Pyr_E} \xrightarrow{k_{cat}[\mathrm{E{\cdot}NAD^+}]} \mathrm{E{\cdot}NAD{-}Pyr} \qquad (1)$$

In this section we show (a) how such a process can provide an explanation for the observation that the rate of the adduct reaction is less than first order with respect to enzyme concentration (Griffin and Criddle, 1970) without invoking the tetramer-to-monomer dissociation step proposed by these workers; (b) how a modification of eq 1 can be used to rationalize the results of Sugrobova *et al.* (1972), as well as additional results described herein; and (c) how eq 1 can be tested experimentally.

There are two limiting kinetic cases for processes proceeding according to eq 1 that are pertinent. (a) If the first reactant, $\mathrm{Pyr_K}$, is in large excess and the interconversion, $\mathrm{Pyr_K} \rightleftharpoons \mathrm{Pyr_E}$, is rapid with respect to the second step, *i.e.* if [$\mathrm{Pyr_E}$] remains constant at its equilibrium value, the rate of appearance of the product, E·NAD-Pyr, will be first order with respect to [E·NAD$^+$]. (b) If the rate of conversion of $\mathrm{Pyr_K}$ to $\mathrm{Pyr_E}$ is much slower than the rate of the second step, and if any $\mathrm{Pyr_E}$ formed reacts immediately to give product, *i.e.*, $k_{cat} \gg k_2$, the appearance of product will be zero order with respect to [E·NAD$^+$]. In addition to these two limiting cases, there are a variety of intermediate cases in which neither step is limiting. In such cases the apparent order of the reaction will be between zero and first order, and the initial velocity will be a nonlinear function of [E·NAD$^+$]. Furthermore, if conditions are such that the initial velocity is *less than first order* with respect to [E·NAD$^+$], an increase in the rate of the enolization step should increase the initial velocity of the adduct reaction. By contrast, if conditions are such that the reaction is strictly first order with respect to [E·NAD$^+$], the rate will be unaffected by an acceleration of the enolization step, as long as the concentration of $\mathrm{Pyr_E}$ remains at its equilibrium value.

General base catalysis of the enolization of ketones by buffers is a well-known phenomenon (Jencks, 1969). Hence, the addition of a buffer to the reaction of Pyr and E·NAD$^+$ will accelerate the enolization without altering the equilibrium concentration of $\mathrm{Pyr_E}$. Thus, the status of the keto–enol interconversion during the adduct reaction can be determined by varying the buffer concentration (at constant pH).

The manner in which the buffer is expected to enter into the reaction is shown in eq 2. Although some of our results cannot

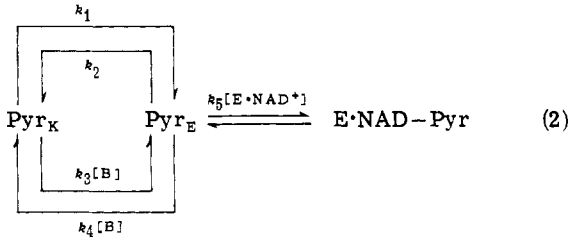

(2)

be rationalized with eq 2, under certain conditions (constant pH, buffer, and pyruvate concentrations) the rate expression for eq 2 does hold. Hence, this equation will be used as a starting point for analyzing the results presented herein.

The iodination of pyruvate proceeds in a manner analogous to eq 2 and provides a useful comparison with the adduct reaction (eq 3). Iodination is a zero-order process (relative to I_2)

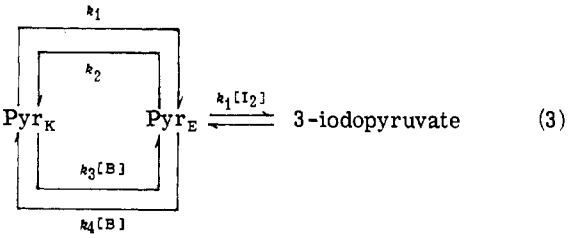

(3)

under all experimental conditions studied (Albery *et al.*, 1965); hence, the reaction must be in the steady state, and the velocity equation is easily derived (eq 4). Here, K_{enol} is the equilibrium

$$\frac{d[I_2]}{dt} = -\frac{[\mathrm{Pyr_K}]}{\dfrac{1}{k_1 K_{enol}[I_2]} + \dfrac{1}{k_1 + k_3[B]}} \qquad (4)$$

constant for enolization of pyruvate, and k_1 is the bimolecular rate constant for the reaction of iodine and pyruvate-enol. Furthermore, the first denominator term in eq 4, which contains [I_2], must be negligible relative to the second denominator term since the iodination is zero order; hence, eq 4 simplifies to

$$\frac{d[I_2]}{dt} = -(k_1 + k_3[B])[\mathrm{Pyr_K}] \qquad (5)$$

Equation 5 indicates that the rate constants for the enolization of pyruvate in the presence and absence of buffer, k_3 and k_1, respectively, can be determined from plots of the velocity of the iodination reaction against buffer concentration.

The rate equation for the reaction of E·NAD$^+$ with pyruvate in eq 2 can be formulated in a manner analogous with eq 5, except the concentration of E·NAD$^+$ replaces the iodine concentration and k_5 represents an apparent bimolecular rate constant for the reaction of E·NAD$^+$ and $\mathrm{Pyr_E}$

$$\frac{d[\text{adduct}]}{dt} = -\frac{d[\mathrm{E{\cdot}NAD^+}]}{dt} = \frac{[\mathrm{Pyr_K}]}{\dfrac{1}{k_5 K_{enol}[\mathrm{E{\cdot}NAD^+}]} + \dfrac{1}{k_1 + k_3[B]}} \qquad (6)$$

A basic assumption in this derivation is that the reaction closely approximates a steady-state process, as does the iodination reaction, before a significant amount of product appears. The validity of this assumption for the present system is supported by numerical integration of the differential equations for the adduct reaction with provisional estimates of the various rate constants (see Results section). The reciprocal form of eq 6 indicates that a double reciprocal plot of the initial rate of the adduct reaction against the initial E·NAD$^+$ concentration should be linear, with a slope of $(k_5 K_{enol}[\mathrm{Pyr_K}])^{-1}$ and a y intercept of $((k_1 + k_3[B])[\mathrm{Pyr_K}])^{-1}$

$$\left(\frac{d[\text{adduct}]}{dt}\right)^{-1} = \frac{1}{k_5 K_{enol}[\mathrm{Pyr_K}][\mathrm{E{\cdot}NAD^+}]} + \frac{1}{(k_1 + k_3[B])[\mathrm{Pyr_K}]} \qquad (7)$$

Moreover, replots of the reciprocal of the intercepts against the buffer concentration can be used to evaluate k_1 and k_3. Alternately, k_1 and k_3 can be obtained by fitting progress curves for the entire adduct reaction (see Experimental Section) to the in-

tegrated form of eq 7 (eq 10) by nonlinear regression analysis. Since the first step in the enzymatic reaction (eq 2) is the same as the first step in the iodination reaction (eq 3), a comparison of the calculated values of k_1 and k_3 for the enzymatic reaction with the corresponding values for the iodination reaction should substantiate the presumed identity of these steps.

Experimental Section

Materials

Grade III samples of NAD^+, NADH, dithiothreitol, sodium oxalacetate, and sodium oxamate from Sigma and sodium pyruvate from Nutritional Biochemicals were used without further purification; solutions of these were prepared and, where necessary, adjusted to pH 7 immediately before use. Dogfish M_4 LDH was purified by the method of Wassarman and Lentz (1971). Its activity was 90–95% of the maximum value (2400 optical density (OD) units mg^{-1} min^{-1}) obtained for the dogfish enzyme (see Standard Assay section). It was stored as an ammonium sulfate suspension and stock solutions were prepared by dialyzing the suspension against several changes of sodium phosphate buffer (pH 7.0) at 4° (μ = 0.15). Solutions thus produced were rapidly dialyzed[3] against four changes of 0.15 M sodium chloride (45 min each) and carefully adjusted to pH 7.0 with small aliquots of 0.01 N hydrochloric acid or sodium hydroxide before use. A concentration of 1×10^{-4} M dithiothreitol was maintained throughout.

Methods

Spectral Studies. The E·NAD–Pyr complex was examined spectrally by using tandem-mix optical cells; total pathlength, 0.875 cm. One side of both sample and reference cells contained pyruvate and the other enzyme; the concentrations of NAD^+, buffer, and dithiothreitol were the same for all compartments. After mixing the contents of the sample cell the resultant spectrum relative to the unmixed reference cell was obtained with a Cary 15 spectrophotometer after no further absorbance changes occurred. The spectrum was "washed out" by mixing the contents of the reference cell; if the washout spectrum was significantly different from the original base line, the experiment was discarded.

Standard Assay. Routine assays were performed at room temperature (23°) by using 2.9 ml of 0.1 M sodium phosphate (pH 7.5), containing 3.3×10^{-4} M pyruvate and 1.3×10^{-4} M NADH. Assays were initiated by the addition of 0.1 ml of enzyme and followed by monitoring the absorption band of NADH at 340 nm with a recording spectrophotometer.

Adduct Reaction. The rate of the adduct reaction as a function of phosphate and enzyme concentrations was measured by following the appearance of an absorption band at 325 nm with a Zeiss monochromator, a Gilford OD converter, and a Honeywell 19K recorder. In some studies the reaction mixture, 0.55 ml, containing the appropriate concentrations of enzyme, NAD^+, dithiothreitol, and phosphate buffer (pH 7.0), at an ionic strength of 0.2, was preequilibrated by using a water-cooled cell holder at 15°, and 50 μl of pyruvate (0.24 M) at 15° was added to initiate the reaction. In other studies, tandem-mix cells were used in the same way as described for the spectral studies. In such cases the concentrations of NAD^+, dithiothreitol, and buffer were the same in all cell compartments; the enzyme and the pyruvate were placed on opposite sides of the cells. The pH of each reaction mixture (except those without buffer) was checked after completion of the reaction; it did not vary during the reaction. The concentration of the adduct complex that was produced was calculated from the observed absorption, based on an extinction coefficient of 7700 M^{-1} cm^{-1} (Griffin and Criddle, 1970).

Numerical Methods. Initial slopes of the product-time curves for the adduct reaction were obtained by extrapolating plots of $[P]/t$ against t to $t = 0$ (Alberty and Koerber, 1957), using a straight line drawn by eye.

The values of all constants in linear equations were obtained by standard least-squares procedures; a CDC 6500 computer was used. The values of all constants in nonlinear equations were obtained by means of a revised version of the SHARE program no. 3094 (nonlinear weighted regression),[4] which adjusts values of the constants in a model to minimize the sums of the squares of the deviations between the observed values and the values of the dependent variable calculated from the model.

Values for the constants in the integrated rate equation for the adduct reaction (eq 10) were estimated by using the above nonlinear regression program. Since the integrated function could be solved directly only in terms of time, time was used as the dependent variable. Thus, the values of the change in absorbance (which is proportional to the adduct complex concentration) were assumed to be exact and the time required to produce this absorbance change, inexact. In order to calculate the values of the constants in eq 10 by means of the above program, the variances for the time required to produce each absorbance change, t, must be known.[5] Since the product-time curves for this reaction are nonlinear (see Figure 6) the variance in t for the ith point, $\sigma_{t_i}^2$, is not constant; however, variances can be calculated as follows[6]

$$\sigma_{t_i}^2 = (\mathrm{d}[f(A_i)])^2 \sigma_{A_i}^2 \qquad (8)$$

Here A_i is the difference in absorbance between that observed at t_0 and that at t_i (the independent variable) and $\sigma_{A_i}^2$ is its variance, which is assumed to be constant. Since only relative values of the weights are required, and since $f(A_i)$ is given by eq 10, weights can be calculated from the extinction coefficient for the adduct complex ϵ_{AC} and following relationship

$$wt_i \propto \sigma_{t_i}^{-2} \propto \left[\frac{1}{(k_1 + k_3[\mathrm{B}])[\mathrm{Pyr_K}]} + \frac{\epsilon_{AC}}{k_5 K_{enol}[\mathrm{Pyr_K}](A_\infty - A_i)} \right]^{-2} \qquad (9)$$

The weights calculated for t_i values in the initial phase of the reaction (<10%) were approximately 100-fold larger than those near the end of the reaction (>90%).

Results

Spectrum of the Adduct Complex. The spectrum (Figure 1) of the adduct complex of dogfish M_4 LDH at pH 7.0 was obtained by measuring absorbance differences in the manner described in the Experimental Section after mixing LDH, NAD^+, and pyruvate and allowing sufficient time for comple-

[3] Rapid dialysis was achieved by restricting the depth of the liquid layer on the inside of the dialysis tubing to about 1 mm by inserting a glass rod with a diameter approximately 2 mm less than that of the tubing.

[4] This program was written by D. W. Marquardt, revised by H. D. Susman, and obtained from the Purdue University Computer Center.

[5] If the values of the dependent variable (time) do not have a constant variance they must be individually weighted.

[6] In general, satisfactory weights can be obtained from the inverse of the variance associated with each point, or from the inverse of any function which yields values directly proportional to the variances (Perrin, 1970).

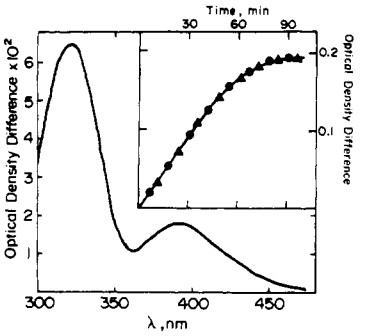

FIGURE 1: Spectrum of the adduct complex. The difference in absorbance between E·NAD$^+$ plus pyruvate and the adduct complex plus pyruvate was recorded at 15° by using tandem-mix cells, that initially contained 0.04 M sodium pyruvate, or 6.67×10^{-3} M NAD$^+$ plus 4.4×10^{-6} M LDH in 0.01 M sodium phosphate buffer (pH 7.0) (μ adjusted to 0.2 with sodium chloride). The measured extinction coefficients at 325 and 380 nm are 7700 and 2100 M^{-1} cm^{-1}, respectively. Inset: Comparison of changes in scaled optical density with time at 325 and 380 nm during the adduct reaction. The conditions and initial concentrations were the same as those described above, except that the LDH concentration was 6.5×10^{-6} M. A factor of 3.6 was used to scale the results obtained at 380 nm relative to those at 325 nm (see Results section).

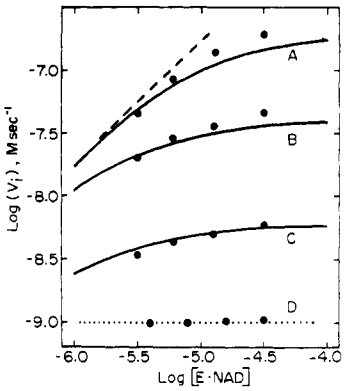

FIGURE 2: Log-log plots showing the effect of imidazole concentration on the relationship between the initial velocity of the adduct reaction and the E·NAD$^+$ concentration. Initial velocities for plots A, B, and C were obtained graphically (see Experimental Section) from the data in Figures 3a, b, and c, respectively (0.225, 0.0375, and 0.00375 M imidazole). Initial velocities for plot D were obtained by direct measurement of the linear phase in plots of optical density *vs.* time. The solid lines were calculated from eq 6 by using values for $10^6(k_1 + k_3[B])$ of 5.3, 2.15, and 0.32 for plots A, B, and C, respectively, as well as the k_5 values in Table I for 0.225, 0.0375, and 0.00375 M imidazole. The dashed and dotted lines represent the expected relationships between initial velocity and E·NAD$^+$ concentration for zero- and pseudo-first-order reactions, respectively.

tion of the reaction (see below). The recorded spectrum actually is a difference spectrum although the absorbances of E·NAD$^+$ and of pyruvate are insignificant over most of the region shown. The wavelength maxima of the peaks in this spectrum, 325 and 380 nm, are the same as those observed for the adduct complex of rabbit muscle LDH (Griffin and Criddle, 1970), as is the molar extinction coefficient at 325 nm, 7700 M^{-1} cm^{-1}; hence, the same adduct probably is produced by both enzymes. In a separate experiment the increment in absorbance at the maxima of the two peaks was followed as a function of time. The results are shown in Figure 1, inset. Since the absorbance at 325 nm is 3.6-fold more intense than that at 380 nm, the absorbance changes at the latter wavelength were multiplied by 3.6 before plotting. Clearly, the two peaks in the difference spectrum are produced either by a single entity, or if not, by multiple entities whose formation is closely linked.[7] Sugrobova *et al.* (1972) observe a similar result with pig M_4 LDH. Although either maximum might be used to follow the formation of the adduct complex, the 325-nm maximum is used exclusively herein because of its larger extinction coefficient.

Calculation of Constants. Concentrations of E·NAD$^+$ were calculated on the basis of a monomer molecular weight of 35,000 (Allison *et al.*, 1969) and thus were equal to four times the tetramer concentration. In addition, a correction factor of 0.9–0.95 also was used since the specific activities of our LDH preparations were about 5–10% low (see Experimental Section). Constants related to the adduct reaction were calculated by assuming that the adduct reaction goes to completion and that the complex does not significantly dissociate under the conditions studied. These are reasonable assumptions since (a) the spectral changes produced by the adduct reaction become constant with time as the accompanying inhibition achieves a value of essentially 100%, and (b) the final absorbance is directly proportional to the initial [E·NAD$^+$] employed. Concentrations of the adduct complex at intermediate reaction times were calculated by using the extinction coefficient at 325 nm noted above.

Effect of Buffer Type on the Rate of the Adduct Reaction. Equation 6 indicates that the initial rate of the adduct reaction should be sensitive to buffer type (as well as buffer concentration), if the enol form of pyruvate is not at its equilibrium concentration during the reaction. This was, in fact, observed with imidazole, Tris, phosphate, phosphate plus acetate, and pyridine buffers (2 mM free base (pH 7); μ = 0.15—data not shown). With the nitrogen bases the initial rates increased with increasing base strength, and the oxygen base, phosphate dianion, was a substantially less efficient catalyst than a nitrogen base with a similar pK_a, imidazole. Such trends are expected if a general base catalyzed removal of a proton from a carbon acid (such as pyruvate) plays a part in the rate-determining step for the adduct reaction (Jencks, 1969).[8]

Apparent Order of the Adduct Reaction in the Presence and Absence of Buffer. To investigate the relationship between buffer concentration and the rate of the adduct reaction, both buffer and E·NAD$^+$ concentrations were varied at pH 7.0 and constant ionic strength. Figure 2 shows plots of the initial rate of the adduct reaction against the E·NAD$^+$ concentration on a log–log scale at three different imidazole concentrations, as well as in the absence of buffer other than that provided by the enzyme itself. The observed initial velocities are sensitive to both [E·NAD$^+$] and [buffer] in the manner required by eq 6, in that the apparent order of the reaction with respect to E·NAD$^+$ (*i.e.*, the slope of a curve at a given E·NAD$^+$ concentration) approaches first order (dotted line) at high concentrations of buffer and low concentrations of E·NAD$^+$ (curve A), and zero order (dashed line) in the absence of buffer (curve D) at all E·NAD$^+$ concentrations used. The solid lines in this figure are calculated from eq 6 and the values for k_1, k_3, and k_5 obtained below.

[7] The product or products that produce the characteristic spectrum of the adduct complex involve a chromophore with a covalent bond between the 4 position of the nicotinamide ring of NAD$^+$ and the methyl carbon of pyruvate (Everse *et al.*, 1971a; Arnold and Kaplan, 1974).

[8] Since general base catalyzed enolization of ketones usually is much more efficient than the corresponding general acid catalyzed process, we assume that the latter type of process does not contribute significantly under the conditions used, pH 7.0.

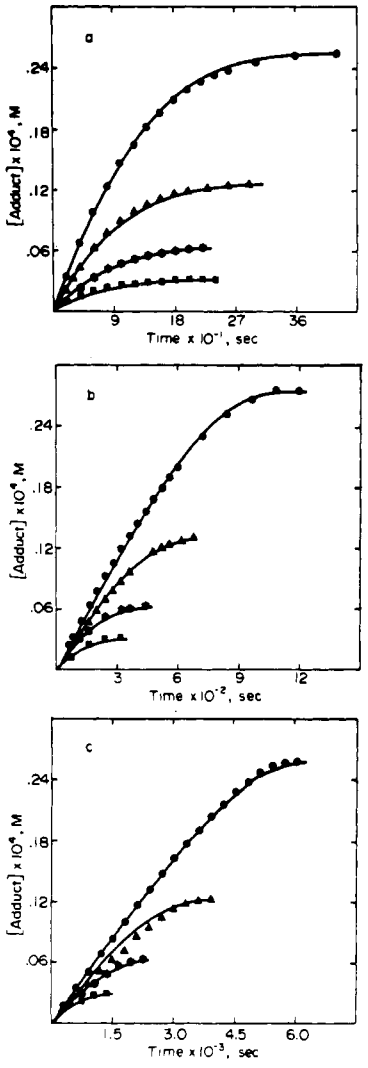

FIGURE 3: The effect of enzyme and imidazole concentration on the rate of the adduct reaction. Conditions and initial concentrations were the same as those indicated in the legend of Figure 1 except for the ionic strength (0.15), and the concentrations of imidazole and of LDH. These were as follows: imidazole: (a) 0.225 M; (b) 0.0375 M; and (c) 0.00375 M; LDH: 2.8×10^{-5} M (●); 1.4×10^{-5} M (▲); 7×10^{-6} M (●); 3.5×10^{-6} M (■). The solid lines in this figure were calculated from eq 10 by using the values of the constants listed in the Figure 2 legend.

Buffer Catalysis of the Adduct Reaction: Evaluation of the Rate Constants for the Imidazole- and Phosphate-Catalyzed Processes. The values of the rate constants, k_1, k_3, and k_5, for the imidazole-catalyzed adduct reaction were determined both from plots of the initial velocities obtained graphically (see Experimental Section) from the product-time plots in Figure 3, and by a numerical regression analysis of data from the entire course of these reactions. The use of alternative methods of calculating the values of constants from the same data serves as an indication of possible deviations from the steady state, since these procedures differ substantially in their dependence on initial data points where such deviations should be the greatest (see below).

The rate expression for the reaction in eq 2 requires that a linear relationship exist between the reciprocal of the initial velocity of adduct formation and the reciprocal of the E·NAD$^+$ concentration (see Theory section). Figure 4 verifies this requirement at three different imidazole concentrations. According to eq 7, the reciprocals of the vertical intercepts in Figure 4

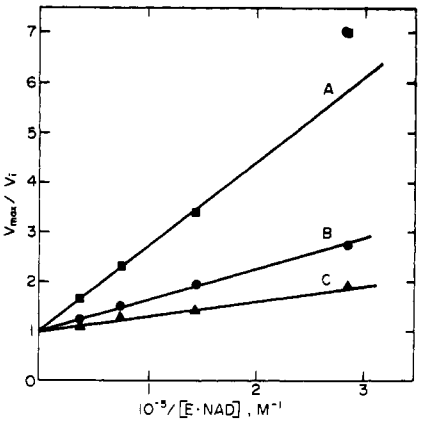

FIGURE 4: Scaled double reciprocal plots of initial velocity of the adduct reaction and E·NAD$^+$ concentration for evaluating k_1 and k_3 at different imidazole concentrations. The scaling factors are the vertical intercepts (V_{max}) at each buffer concentration; these are as follows: (A) 0.14 ΔOD unit/min; (B) 0.026 ΔOD unit/min; (C) 0.003 ΔOD unit/min. The initial velocities for A, B, and C were calculated from the data in the corresponding Figure 3 plots and were the same as those used in Figure 2. Calculated regression lines are shown (solid lines).

(see Figure legend) should be equal to $(k_1 + k_3[B])[Pyr_K]$. A replot of these intercepts against imidazole concentration (calculated as the free base, [B]) is shown in Figure 5 (●) and is linear, as expected ($r > 0.999$). Values of k_1 and k_3 were estimated from the intercept and slope, respectively, of the line in Figure 5 and values of k_5 were calculated from the reciprocals of the slopes of the lines in Figure 4 (see eq 7). These values are noted below.

In order to evaluate the above constants from the entire product-time curves (Figure 3) the integrated form of eq 6 was used in separate weighted regression analyses for Figure 3a–c (see Experimental Section) (eq 10). Here [P] and $[P]_\infty$ are the

$$t = \frac{[P]}{(k_1 + k_3[B])[Pyr_K]} + \frac{1}{k_5 K_{enol}[Pyr_K]} \log \frac{[P_\infty]}{[P_\infty] - [P]} \quad (10)$$

concentrations of adduct complex at time, t, and at the end point, respectively, and the constants are the same as those in eq 6. Values obtained for the reciprocal coefficient of the first term in eq 10, *viz.*, $(k_1 + k_3[B])[Pyr_K]$, are essentially the

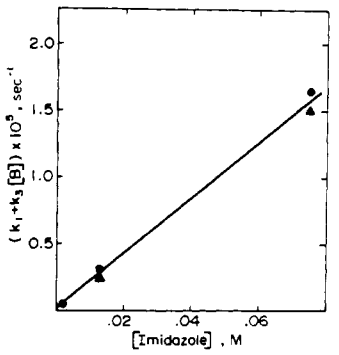

FIGURE 5: The effect of imidazole on the pseudo-first-order rate constant, $k_1 + k_3[B]$, for enolization of pyruvate as evaluated by the graphical and numerical analyses; (●) values of the reciprocal of the coefficient of the first term in eq 7, *i.e.*, the y intercepts in Figure 3; (▲) values from the numerical analysis of the reciprocal coefficient of the first term in eq 10 (*i.e.*, linear in [P]). Average values for k_1 and k_3 obtained by regression analysis of both sets of data are $0.4 \pm 1.5 \times 10^{-7}$ sec^{-1} and $2.5 \pm 0.12 \times 10^{-4}$ M^{-1} sec^{-1}, respectively.

TABLE I: Values for k_5 in Equation 2.[a]

Buffer	Concn (M)	$10^{-5} \times k_5$ (M^{-1} sec^{-1})
Imidazole	0.225	2.0 ± 0.1
	0.0375	1.3 ± 0.1
	0.00375	0.3 ± 0.02
Phosphate	0.1	1.9 ± 0.1
	0.05	1.3 ± 0.1
	0.01	0.2 ± 0.02

[a] Values were obtained by the regression analysis (see Results section) of the adduct reaction curves in Figure 6 (imidazole buffer) and similar data (not shown) for the reaction in the presence of phosphate buffer.

same as those determined by the above graphical analysis (see below), and also are linearly related to buffer concentration ($r > 0.999$) ((▲), Figure 5). Values of k_5 (see below), obtained by both procedures, also are essentially the same. In addition, the solid lines in Figure 3 were calculated by using the integrated rate equation (eq 10) and the numerically determined values of k_1, k_3, and k_5. In view of the wide concentration range investigated, the fit of these lines to the experimental data (Figure 3) is quite reasonable. Thus, the rate-determining step is sensitive to both buffer type and concentration, and the entire course of the adduct reaction at constant buffer and pyruvate concentrations is adequately described by eq 10. Hence, it seems reasonable to conclude that formation of the adduct reaction involves the enolization of pyruvate.

The value of k_3 for imidazole, obtained from the regression line calculated by using both sets of data in Figure 5, is (2.15 ± 0.12) × 10^{-4} M^{-1} sec^{-1}; k_1 evaluated similarly was not significantly different from zero, but may be taken as equal to or less than 3 × 10^{-7} sec^{-1} (twice the standard error of the estimate). Values for k_5 obtained from the numerical regression analysis are given in Table I at the three different concentrations of imidazole that were employed in Figure 3; a value for K_{enol} of 4 × 10^{-6} (see below) was used to calculate k_5 from the coefficient of the logarithmic term in eq 10. The variation of k_5 with buffer concentration will be considered in the Discussion section, but this variation in no way invalidates the conclusions drawn in the Results section based on measurements at a fixed buffer concentration.

Product-time plots (not shown) analogous to those in Figure 3 also were obtained by using inorganic phosphate (0.006–0.1 M) as the buffer, and were analyzed by the numerical regression procedure in conjunction with eq 10. Again, reciprocal coefficients of the first term in eq 10 also were linearly related to buffer concentration. The plot of these values against phosphate concentration, which is similar to Figure 5, is not shown, but $r > 0.999$; k_1 = (5 ± 2) × 10^{-8} sec^{-1}; and k_3 = (4.1 ± 0.4) × 10^{-5} M^{-1} sec^{-1} (calculated for the dianion). Values of k_1 and k_3 determined by the graphical method (not shown) also were indistinguishable from these values. Thus, phosphate (dianion) is somewhat less efficient than imidazole in catalyzing the enolization of pyruvate. Values of k_5 at three different phosphate concentrations were determined as above and are given in Table I.

Rate Constants for the Adduct Reaction in the Absence of Buffer. In order to obtain a more accurate estimate of the value k_1 than obtained by extrapolation of data obtained in the presence of the buffers to zero buffer, *i.e.*, from the y intercept in Figure 5, the rate of the adduct reaction at different [E·NAD$^+$] was measured directly in the absence of buffer (other than that provided by the enzyme itself) at pH 7.0, and the results were analyzed in the manner described above for Figure 4. The value of k_1 from the average of three determinations is (8.2 ± 1.2) × 10^{-8} sec^{-1}. This value is within the range of values for k_1 obtained in the presence of imidazole buffer, ≤3 × 10^{-7} sec^{-1}, and phosphate buffer, (5 ± 2) × 10^{-8} sec^{-1}.

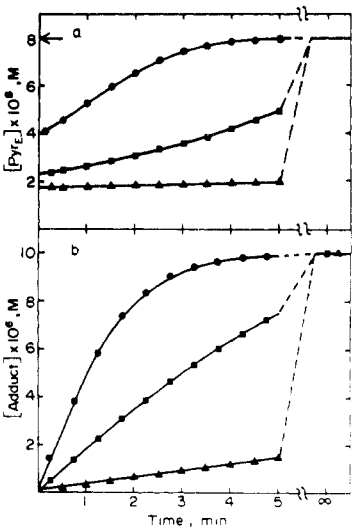

FIGURE 6: Simulation of concentrations of pyruvate enol (a) and adduct complex (b) as a function of time for 0.02 M pyruvate and 10^{-5} M E·NAD$^+$. Details of the method of simulation and the values of the rate constants used are given in the text. The arrow indicates the equilibrium concentration of the enol form of pyruvate based on a value for K_{enol} of 4 × 10^{-6}.

Validation of the Steady-State Approximation for the Adduct Reaction. The validity of the steady-state approximation used in deriving the rate equation (6) for the adduct reaction (eq 2) can be substantiated by an analysis in which the general rate equations with initial conditions analogous to those employed and rate constants in the range of those estimated from the Figure 3 plots for the adduct reaction are numerically integrated. The Runge–Kutta method[9] was used for this procedure with the following parameters: k_1 = 5 × 10^{-8} sec^{-1}; k_3[B] = 1.58 × 10^{-5}, 2.63 × 10^{-6}, or 2.63 × 10^{-7} sec^{-1}; the respective values of k_5K_{enol} were 0.79, 0.53, and 0.11; K_{enol} was taken as 4 × 10^{-6} (see below) and values for k_2 and k_4 were calculated from this value and the above values of k_1 and k_3. The concentrations of E·NAD$^+$ and pyruvate were taken as 1 × 10^{-5} and 0.02 M, respectively. A Pyr$_E$ concentration of 8 × 10^{-8} M (*i.e.*, K_{enol}[Pyr$_K$]) was used to initiate the integration. The integration routine calculated values for the concentrations of adduct complex and [Pyr$_E$] as a function of time. The results are shown in Figure 6. It is important to note that the rapid initial decrease in [Pyr$_E$] (compare y intercepts in a with position of the arrow) and the corresponding "burst" of adduct that is produced during the change in the enol concentration from its equilibrium concentration to that characteristic of the (presumed) steady state are too small to detect under our conditions, *i.e.*, the y intercepts in b are not significantly different from zero on the scale shown or used in the assay. Apparent values for the initial rate of the adduct reaction (d[P]/dt), and

[9] A digital to analog simulator program (MIMIC, modification 1) for solving ordinary differential equations, which was made available by Control Data Corporation through the Purdue University Computer Center, was used to integrate the general rate equations.

TABLE II: Comparison of Changes in Concentration with Time for Enol and Adduct during the "Initial Velocity Phase" of a Simulated Reaction.[a]

$10^5 \times k_3[B]$ (sec^{-1})	$10^8 \times d[Pyr_E]/dt$ ($M\ sec^{-1}$)	$10^{10} \times d[E{\cdot}NAD^+{-}Pyr]/dt$ ($M\ sec^{-1}$)	Ratio
1.58	9.2	2.2	420
0.26	3.0	0.50	600
0.026	0.45	0.13	350

[a] The velocities are obtained from the slope of that portion of the simulated reaction curves (Figure 8) just after the initial burst phase—see Results section.

TABLE III: Comparison of Values of the Rate Constants for Enolization of Pyruvate.[a]

Reaction	Buffer	$10^8 k_1$ (sec^{-1})	$10^5 k_3$[b] ($M^{-1}\ sec^{-1}$)
Iodination	Phosphate	6 ± 2	5.5 ± 0.1
	Tris	5 ± 4	57 ± 1
	None	4 ± 1	
Formation of adduct complex	Phosphate	5 ± 2	4.1 ± 0.4
	Imidazole	<28	14 ± 0.4
	None	8 ± 1	

[a] Standard errors of the estimates are given. Constants are defined in eq 2. [b] Values calculated for the basic forms of imidazole and Tris, and for the phosphate dianion.

the initial change in $[Pyr_E]$ with time, estimated graphically from the slopes of these plots just after the burst phase, appear in Table II. The ratio of these rates, *i.e.*, $d[P]/d[Pyr_K]$, is greater than 100 for three different sets of reaction conditions approximating those in Figure 3. A ratio of this size is both necessary and sufficient to validate the application of the steady-state approximation to equations describing this reaction. In fact, any process that can be described by a scheme analogous to that in eq 2 will be in steady state before a significant fraction of the reactants is converted to products if the initial conditions are analogous to those used and the corresponding rate constants are in the range estimated for the adduct reaction. Hence, if eq 2 describes the adduct reaction, which it apparently does, the latter must be a steady-state process. The similarity in the values of $(k_1 + k_3[B])$ calculated both from initial velocities and from numerical analysis of the entire course of the reaction (see above) also lends support to this conclusion.

Kinetics of the Iodination of Pyruvate. The rate of iodination of pyruvate by iodine in the presence of sodium iodide was measured under the same conditions of ionic strength, pH, and temperature that were used in the adduct reaction, for reasons outlined in the Theory section. The effect of Tris and phosphate buffers on the reaction rate also was assessed and values for the constants k_1 and k_3 (see eq 3) were determined; see Table III. In addition, a value for the pyruvate keto–enol equilibrium constant, K_{enol}, of $4.1 \pm 0.2 \times 10^{-6}$ was obtained by measuring the pre-steady-state burst phase of the iodination reaction at high pyruvate concentrations (1.0 M). Because these studies are analogous to other studies of the iodination reaction (Albery *et al.*, 1965), our studies are described in a Supplemental Section (see paragraph at end of paper regarding supplementary material). The results are consistent with the previously reported data but could not be accurately predicted from those data, because of differences in reaction conditions.

Comparisons of Rate Constants for Reaction of Pyruvate with E·NAD⁺ and with Iodine. Since the enolization of pyruvate is presumed to be rate determining for the reactions in eq 2 and 3, a comparison of the values of the analogous rate constants for the adduct reaction and the iodination reaction was made (see Table III). The average of the values for the first-order rate constant for the uncatalyzed enolization of pyruvate, k_1, determined from iodination experiments conducted both in the presence of phosphate buffer and in the absence of buffer, $5 \times 10^{-8}\ sec^{-1}$, is the same as the value determined from the adduct experiments in the presence of phosphate buffer (and extrapolated to zero buffer) and comparable to the value estimated in the absence of buffer, $8 \times 10^{-8}\ sec^{-1}$. In addition, the values of the second-order rate constants, k_3, which describe the effect of phosphate buffer on the iodination and adduct reactions, are similar (see Table III). Thus, the same buffer-dependent process undoubtedly controls the iodination of pyruvate and the adduct reaction. Since the enol form of pyruvate is the reactant in the iodination process it also must be the reactant in the adduct process.

Discussion

Although there is no apparent chemical similarity between I_2 and the complex of LDH with NAD^+, this study presents compelling evidence that both react in a kinetically similar manner with pyruvate in neutral aqueous solution. In one case the product is iodopyruvate, in the other, the E·NAD–Pyr adduct complex. However, the enolization of pyruvate is an obligatory process prior to the bond-making step in both reactions. In fact, the primary kinetic difference in the two reactions is the much greater reactivity of I_2 relative to $E{\cdot}NAD^+$ toward the enol form of pyruvate, and if the concentration of $E{\cdot}NAD^+$ could be sufficiently elevated to compensate for its reduced reactivity, the observed rate of reaction with pyruvate would be the same for both reagents, *i.e.*, zero order in I_2 or zero order in $E{\cdot}NAD^+$. In fact, at high $E{\cdot}NAD^+$ the initial velocity can approach zero order even at the concentrations of $E{\cdot}NAD^+$ used here (see Figure 2, plot D). However, product–time plots in such studies begin to deviate from linearity much earlier than in the iodination process, because, as $E{\cdot}NAD^+$ is used up, ketonization (the k_2 step in eq 2) begins to compete effectively with the $E{\cdot}NAD^+$ reaction for the enol. Because of this competition the apparent order of the adduct reaction is sensitive to $[E{\cdot}NAD^+]$, whereas the order of the iodination reaction is insensitive to $[I_2]$—at least under the conditions usually used for iodination.

The competition between the ketonization and the $E{\cdot}NAD^+$ reaction also gives rise to a buffer sensitivity that is not apparent in the iodination reaction. Thus, although the *rates* of *both* processes (at constant pH and ionic strength) are sensitive to buffer concentration because of its effect on the $Pyr_E \rightarrow Pyr_K$ step, the *order* of the $E{\cdot}NAD^+$ reaction is also buffer sensitive whereas the order of the iodination reaction is not. Thus, to evaluate the buffer effect in the $E{\cdot}NAD^+$ reaction, one must contend with changing reaction order as well as changing rates. However, after disentangling these two effects, the measured correspondence in the buffer effect of inorganic phosphate, *i.e.*,

general base catalysis by phosphate, on the *rates* of the I_2 and E·NAD$^+$ reactions is quite satisfactory (see Table III and the Results section). In addition, values of the rate constant for the uncatalyzed enolization of pyruvate calculated both from the I_2 and the E·NAD$^+$ reactions are in good agreement (see Results section). Because of this agreement and because of the general success of eq 2 in providing a rationale for the variation in rate of the adduct reaction with E·NAD$^+$ at fixed buffer and pyruvate concentrations (see below), the suggestion of Griffin and Criddle (1970) that dissociation of the tetramer of LDH to form a reactive monomer accounts for these complexities is no longer tenable.

A third difference between the reaction of I_2 and E·NAD$^+$ with pyruvate lies in step 5 of eq 2, *i.e.*, the product-forming step. In the enzymic reaction this step (which actually is a series of steps—see below) also is subject to buffer catalysis which produces the apparent variation in k_5 values seen in Table I (see also below). By contrast, the reaction of I_2 with pyruvate enol is so fast with respect to the formation of the enol that if a buffer effect does influence the rate of the bond-forming step the effect cannot be detected.

The above differences are quantitative in nature and thus are caused by differences in the relative magnitude of rate constants. However, a final difference between iodination and the adduct reaction is one that is common in comparison of enzymic and nonenzymic processes: formation of a complex of the reactants in the enzymic system. In fact, the present study, in conjunction with the results of others (Ozols and Marinetti, 1969; Everse *et al.*, 1971b; Sugrobova *et al.*, 1972), provides strong evidence for the involvement of reactive E·NAD·Pyr$_E$ and unreactive E·NAD·Pyr *ternary* complexes (Burgner, 1973).[10] The first of these complexes also appears in the mechanism proposed by Sugrobova *et al.* (1972) for the adduct reaction, although their mechanism appears to be incorrect with regard to assignment of relative velocities to the various reaction steps.[11] The involvement of the above complexes in the adduct reaction together with a more thorough treatment of the buffer effect on step 5, eq 2, will be the subject of a subsequent paper (J. W. Burgner, II, and W. J. Ray, Jr., manuscript in preparation).

Several *in vitro* studies have been conducted in attempts to assess either the relative importance or biological significance of pyruvate-induced inhibition of LDH *in vivo* (Plagemann *et al.*, 1961; Cahn *et al.*, 1962; Stambaugh and Post, 1966; Vesell and Pool, 1966; Kaplan *et al.*, 1968; Wuntch *et al.*, 1969; Everse *et al.*, 1971a). However, the present results indicate that conclusions drawn from such studies may be open to question. For instance, initial velocity studies have involved conditions where the half-time for the adduct reaction is many minutes and linear product–time plots were observed for several minutes (Zewe and Fromm, 1962; Stambaugh and Post, 1966). In such cases, the observed pyruvate inhibition cannot be produced by the adduct reaction and probably is caused by formation of a ternary E·NAD·Pyr complex analogous to the ternary E·NAD·oxamate complex (Burgner, 1973; J. W. Burgner, II, and W. J. Ray, Jr., manuscript in preparation). In other cases, where the buffer concentration was higher, the adduct complex may contribute to the inhibition of LDH. However, if *true* initial velocities were measured in these studies, the observed inhibition still must result from the ternary E·NAD·Pyr complex, and the *in vivo* importance of the adduct complex may have been significantly underestimated. Thus, the most reasonable approach to an *in vitro* evaluation of the overall inhibition of LDH by pyruvate under "physiological conditions" is to conduct the initial velocity study in the presence of sufficiently high concentrations of amine buffers, *e.g.*, imidazole, to allow the adduct reaction to reach "completion" before a substantial fraction of the pyruvate is used up. An investigation utilizing this procedure currently is in progress.

[10] Tienhaara and Meany (1973) have suggested that the hydrated form of pyruvate is an inhibitor of LDH; hence, the unreactive E·NAD$^+$·pyruvate complex may involve either the hydrated form of pyruvate, the keto form, or both.

[11] It is difficult to deduce precisely what Sugrobova *et al.* (1972) propose with respect to the rate-limiting step in the adduct reaction. In eq 7–10 they indicate that both the enolization step and the bond-forming step are "slow"; however, their arguments in paragraphs 5 and 6 of the Discussion are predicted on the (tacit) assumption that the enolization step in fact is at equilibrium during the adduct reaction. Later, they refer to the two "slow" steps in eq 7–10 and seem to suggest that both contribute to the rate of the reaction, whereas their Abstract notes only that the bond-forming step is slow. In no place do they propose a change in rate-determining step as an explanation of their data, as one might expect if they feel that the rates of their "slow" steps were of comparable magnitude.

Supplementary Material Available

A Supplemental Section will appear following these pages in the microfilm edition of this volume of the journal. Photocopies of the supplementary material from this paper only or microfiche (105 × 148 mm, 24× reduction, negatives) containing all of the supplementary material for the papers in this issue may be obtained from the Journals Department, American Chemical Society, 1155 16th St., N.W., Washington, D. C. 20036. Remit check or money order for $3.00 for photocopy or $2.00 for microfiche, referring to code number BIO-74-4229.

References

Alberty, R. A., and Koerber, B. M. (1957), *J. Amer. Chem. Soc. 79*, 6379.

Albery, W. J., Bell, R. P., and Powell, A. L. (1965), *Trans. Faraday Soc. 61*, 1194.

Allison, W. S., Admiraal, J., and Kaplan, N. O. (1969), *J. Biol. Chem. 244*, 4743.

Arnold, L. J., Jr., and Kaplan, N. O. (1974), *J. Biol. Chem. 249*, 652.

Burgner, J. W., II (1973), Ph.D. Thesis, Purdue University, West Lafayette, Ind.

Cahn, R. D., Kaplan, N. O., Levin, L., and Zwilling, E. (1962), *Science 136*, 962.

DiSabato, G. (1968), *Biochem. Biophys. Res. Commun. 33*, 688.

Everse, J., Barnett, R. E., Thorne, C. J. R., and Kaplan, N. O. (1971a), *Arch. Biochem. Biophys. 143*, 444.

Everse, J., and Kaplan, N. O. (1973), *Advan. Enzymol. Relat. Areas Mol. Biol. 37*, 66.

Everse, J., Zoll, D. C., Kahan, L., and Kaplan, N. O. (1971b), *Bioorg. Chem. 1*, 207.

Griffin, J. H., and Criddle, R. S. (1970), *Biochemistry 9*, 1195.

Gutfreund, H., Cantwell, R., McMurray, D. H., Criddle, R. S., and Hathaway, G. (1968), *Biochem. J. 106*, 683.

Holbrook, J. J., and Gutfreund, H. (1973), *FEBS (Fed. Eur. Biochem. Soc.) Lett. 31*, 157.

Jencks, W. P. (1969), Catalysis in Chemistry and Enzymology, New York, N. Y., McGraw-Hill, pp 229–231.

Kaplan, N. O., Everse, J., and Admiraal, J. (1968), *Ann. N. Y. Acad. Sci. 151*, 400.

Lee, H. A., Cox, R. H., Smith, S. L., and Winer, A. D. (1966), *Fed. Proc., Fed. Amer. Soc. Exp. Biol. 25*, 711.

Lee, H. A., Eisman, G. H., and Winer, A. D. (1965), *Fed. Proc., Fed. Amer. Soc. Exp. Biol. 24*, 667.

Novoa, W. B., Winer, A. D., Glaid, A. J., and Schwert, G. W. (1959), *J. Biol. Chem. 234,* 1143.
Ozols, R. F., and Marinetti, G. V. (1969), *Biochem. Biophys. Res. Commun. 34,* 712.
Perrin, C. L. (1970), Mathematics for Chemists, New York, N. Y., Wiley, p 159.
Plagemann, P. G. W., Gregory, K. F., and Wroblewski, F. (1961), *Biochem. Z. 334,* 37.
Stambaugh, R., and Post, D. (1966), *J. Biol. Chem. 241,* 1462.
Sugrobova, N. P., Kurganov, B. I., Gurevich, V. M., and Yakoviev, V. A. (1972), *Mol. Biol. 6,* 217.
Tienhaara, R., and Meany, J. E. (1973), *Biochemistry 12,* 2067.
Vesell, E. S., and Pool, P. E. (1966), *Proc. Nat. Acad. Sci. U. S. 55,* 756.
Wassarman, P. M., and Lentz, P. J. (1971), *J. Mol. Biol. 60,* 509.
Wuntch, T., Vesell, E. S., and Chen, R. F. (1969), *J. Biol. Chem. 244,* 6100.
Zewe, V., and Fromm, H. J. (1962), *J. Biol. Chem. 237,* 1668.

Mitochondrial Membranes of Inositol-Requiring *Saccharomyces carlsbergensis:* Covalent Binding of a Radioactive Marker to the Outer Membrane†

A. Joanne Bednarz-Prashad‡ and Charles E. Mize*,§

ABSTRACT: Tritium can be bound covalently and specifically to the outer membrane of intact mitochondria from *Saccharomyces carlsbergensis,* providing a sensitive marker for monitoring separation of mitochondrial membranes. Mitochondria are obtained by osmotic shock from *S. carlsbergensis* spheroplasts. They are labeled with tritium by NaB^3H_4 reduction of Schiff bases, formed between externally added pyridoxal phosphate and free amino groups on the surface of the mitochondrion. The mitochondria rupture when sonicated and yield inner and outer membranes which separate on sucrose density gradients. Outer membrane fractions from the gradient appear at 28–35% sucrose and contain 70% of the monoamine oxidase activity, 90% of the tritium radioactivity, and essentially no cytochrome *c* oxidase activity. Inner membrane fractions from the gradient appear at 54–68% sucrose and contain 90% of the cytochrome *c* oxidase and 27% of the monoamine oxidase activity.

The study of mitochondrial structure, composition, and function is basically dependent upon an adequate separation of the mitochondria from the cells, and upon successful fractionation of the mitochondria into their component parts (inner and outer membranes, and matrix fractions). Mammalian mitochondria are easily accessible and are generally prepared by a variety of differential centrifugation procedures (Parsons *et al.,* 1967; Schnaitman and Greenawalt, 1968; de Duve *et al.,* 1955). Yeast mitochondria are less accessible due to the heavy cell wall. They can be prepared by breaking the cells in a Braun homogenizer (Henson *et al.,* 1968) or by homogenization or osmotic shock of the spheroplasted cells (Hutchison and Hartwell, 1967). The separation of mitochondrial inner and outer membranes can be accomplished by osmotic shock (Bandlow, 1972), digitonin treatment (Schnaitman *et al.,* 1967), or by sonication (Whereat *et al.,* 1969), all usually followed by sucrose density gradient fractionation.

All of the above procedures are monitored for success on the basis of enzymatic activity for marker enzymes of the mitochondrion and its component membranes and compartments. As pointed out by Huber and Morrison (1973), difficulties arise when the exact location of these enzymes is not clear. This is especially true with regard to the outer membrane. In addition, known marker enzymes (such as the monoamine oxidase) may be quite low in activity, or appear in mammalian mitochondria but, perhaps, not in yeast mitochondria (Bandlow, 1972). Problems such as these may be circumvented by the use of nonenzymatic markers, such as a radioactive label. The addition of a tritium label to the outer surface of an intact mitochondrion can be accomplished by reduction of Schiff bases with Na^3BH_4. The Schiff base formation between free amino groups on the mitochondrion and pyridoxal phosphate, and the subsequent gentle reduction with sodium borotritide, proceeds under physiological conditions and apparently does not affect mitochondrial function. This procedure was first described by Cooper and Reich (1972) for labeling isolated proteins and was subsequently used by Rifkin *et al.* (1972) for labeling the outer surface of influenza viruses.

Materials and Methods

Chemicals and Chemical Methods. Ultrapure sucrose for density gradients and tris(hydroxymethyl)aminomethane (Trizma Base) were obtained from Sigma Chemical Co. (St. Louis, Mo.); glusulase, Endo Laboratories (Garden City, N. Y.); and pyridoxal phosphate, Calbiochem (La Jolla, Calif.). [1-^{14}C]Stearic acid (56 Ci/mol) was obtained from Amersham/Searle (Des Plaines, Ill.); benzylamine, Eastman Kodak Chemicals (Rochester, N. Y.); cytochrome *c* (horse heart, crystalline), Boehringer Mannheim Corp. (New York, N. Y.). Sodium boro[^{3}H]hydride (138 Ci/mol) was obtained from

† From the Departments of Biochemistry and Pediatrics, University of Texas Health Science Center (Southwestern) at Dallas, Dallas, Texas 75235. *Received April 1, 1974.* Supported by Robert A. Welch Foundation Grant 1-454 and U. S. Public Health Service Grant 5 TO1 AM 05571. A preliminary report of part of these findings has been published (Bednarz and Mize, 1973).
‡ Robert A. Welch Foundation Postdoctoral Fellow.
§ U. S. Public Health Service Career Development Awardee.